Annals of Glaciology 25 1997

The effect of sea-ice parameterizations on the simulation of the Arctic ice pack

Stephen J. Vavrus
Center for Climatic Research, 1225 West Dayton Street, University of Wisconsin, Madison, WI 53706, U.S.A.

ABSTRACT. A one-dimensional (1-D), thermodynamic sea-ice model with parameterized ice dynamics is coupled to a mixed-layer ocean model and driven with prescribed atmospheric forcings for the central Arctic. The model is used to calculate the sensitivity of the ice pack to various parameterizations that have traditionally been neglected or considered only implicitly in large-scale sea-ice models. The model includes melt ponds, leads (with summertime stratification), an ice-export term, a stability-dependent air–sea heat-exchange coefficient, a prognostic ocean–ice heat exchange, a crude ice-thickness distribution, and a sophisticated albedo parameterization.

The ice pack is sensitive to the partitioning of solar energy between lateral melting and mixed-layer warming, with the most realistic simulations occurring when the heat is nearly evenly divided between these two processes. Conversely, ice thickness and coverage are fairly insensitive to the amount of lateral mixing within the upper ocean, vertical mixing within leads, and to the partitioning of mixed-layer heat content between warming the water and melting the ice bottom. The ice concentration during summer is strongly dependent on the assumed ice-thickness distribution: the amount of open water during summer is less than half the size of the empirically based distribution used here, compared with one in which ice floes are distributed uniformly across a range of thicknesses.

INTRODUCTION

A variety of recent research has identified the polar regions as especially sensitive components of the global-climate system. Modeling experiments with general circulation models (GCMs) involving future scenarios with doubled CO_2 concentrations and past climates under altered orbital configurations have shown that high latitudes respond most strongly to global-climate changes (e.g. Mitchell and others, 1990; Kutzbach and others, 1991). Paleoenvironmental evidence supports these results and suggests that polar climates vary widely on time-scales of decades to millions of years (e.g. Alley, 1995). As a consequence of this extreme sensitivity and its global implications, it is essential that polar regions are modeled in order to diagnose and predict their role in future global change.

One of the most robust results of GCM simulations with increased atmospheric CO_2 is the pronounced poleward amplification of warming. This result has been illustrated by a variety of experiments, ranging in sophistication from instantaneous CO_2 doubling using coupled atmosphere–static mixed-layer ocean models (e.g. Washington and Meehl, 1984) and coupled atmosphere–mixed-layer models with prescribed oceanic heat transport (e.g. Wilson and Mitchell, 1987), to transient CO_2 doubling using fully coupled atmosphere–ocean models (e.g. Manabe and others, 1991). Such sensitivity tests have found that the high-latitude warming due to increased CO_2 is 2–3 times the global average. These studies have attributed the enhanced sensitivity of both polar regions to the greatly increased air–sea heat transfer when sea ice and snow cover are reduced.

The role of sea ice in amplifying the high-latitude climatic response deserves particular attention, because of the direct thermodynamic and hydrologic effects of sea ice on both the atmosphere (by regulating the air–sea exchange of heat and moisture) and the ocean (by controlling salt fluxes into the mixed layer). Unfortunately, sea-ice models are known to be sensitive to numerous uncertain parameters and processes, such as the parameterization of leads (Vavrus, 1995), surface albedo (Shine and Henderson-Sellers, 1985), ocean–ice heat flux (Maykut and Untersteiner, 1971), and ice dynamics (Hibler, 1984). Sea-ice simulations may also depend on other mechanisms even more difficult to quantify, such as the partitioning of solar energy between oceanic warming and ice melting (Maykut and Perovich, 1987), vertical and lateral mixing of water within leads and beneath ice floes (Perovich and Maykut, 1990), and the presence of thin and thick ice floes within an ice pack (Curry and others, 1995).

The goal of this study is to test several parameterizations in a sea-ice model to evaluate the importance of various processes that could affect the simulation of Arctic ice cover, and to estimate the most likely behavior of the actual ice–ocean system by comparing simulations with observations. The emphasis here is to improve sea-ice simulations in large-scale climate models, rather than in high-resolution regional and operational models.

MODEL DESCRIPTION

An overview of the essential components of the model is given here. The model is a one-dimensional (1-D) representation of the growth and decay of sea ice at a single point representative of the central Arctic; there is no latitudinal or longitudinal variation. The ice cover is underlain by a

https://doi.org/10.3189/S0260305500013720 Published online by Cambridge University Press

50 m mixed layer that is completely decoupled from the deep ocean, so that none of the warm Atlantic water at depth can reach the ice base. This decoupling is justified by the central Arctic's extreme stratification, which has been confirmed by a number of studies (e.g. McPhee and Untersteiner, 1982; Morrison and Smith, 1981). The skeletal thermodynamics of the model are described in Semtner (1976), Parkinson and Washington (1979), and Ebert and Curry (1993). The 0-layer approximation of Semtner (1976) is used for the diffusive heat flux through the ice. The growth and decay of leads are a combination of the approaches used by Parkinson and Washington (1979) and Ebert and Curry (1993). The model also includes melt ponds, the depths of which follow the approach of Ebert and Curry (1993), but the areal extent of which is a linear function of the surface melt rate to produce a seasonal cycle consistent with observed estimates (Barry, 1983). As in Ebert and Curry (1993), there is a prescribed ice-export term, which forces ice divergence at all times of the year. The basal heat flux is prognostic, and is determined by the input of solar energy into the mixed layer, with a temperature and turbulence dependence described by McPhee (1992).

An alternate model version allows the solar-energy input to be partitioned in a prescribed manner between the warming of the mixed layer and lateral melting. During melting conditions, there is a prescribed ice-thickness distribution within the pack, to account for the vertical meltoff of thin ice and the different lateral melting rates of thin and thick ice. Unlike previous models, which assume a uniform distribution of thin and thick ice floes (e.g. Hibler, 1979; Harvey, 1988), the ice distribution here is assumed to be triangularly shaped between 0 and twice the mean ice thickness, giving the smallest amounts of very thin and very thick ice and the largest amounts of ice near the mean thickness. This choice of distribution is more consistent with measured thickness distributions of Arctic sea ice (e.g. Tucker and others, 1992). A vertical-mixing coefficient within leads was used (set to 50% of complete mixing in the control case) during the melt season to account for the assumed stratification between the upper lead (water surface to ice bottom) and the lower lead (bottom of ice to mixed-layer depth of 50 m). A lateral-mixing coefficient (set to 100% of possible mixing in the control case) adjusts the amount of mixing between the lower lead and the water beneath the ice. The ice and snow albedos are functions of cloud cover, surface temperature and thickness and are based on a variety of observational estimates and theoretical calculations (Grenfell and Maykut, 1977; Grenfell, 1979; Shine and Henderson-Sellers, 1985). The rate of turbulent heat transfer from the air to the ice, snow or water depends on the atmospheric stability, as described by Ebert and Curry (1993). The model is forced by the atmospheric dataset published there, except for snowfall, for which Maykut and Untersteiner's (1971) values are used.

RESULTS OF CONTROL SIMULATION

Using the atmospheric forcings for the central Arctic described earlier, the model was run to equilibrium using the control settings of the lateral- and vertical-mixing coefficients, the ice-thickness distribution, and the basal heat flux formula (Table 1). The simulated seasonal and annually averaged sea-ice characteristics compare well with observations, with respect to ice thickness and lead fraction (Fig. 1), basal heat flux, melt-pond fraction, and ice-surface temperature. A comparison with other sea ice models' sensitivity to infrared heat flux perturbations (Curry and others, 1995) shows that this model is comparably sensitive to those of Ebert and Curry (1993), Maykut and Untersteiner (1971), and Semtner (1976).

Table 1. Parameters used in the control simulation

Lateral-mixing efficiency	1
Vertical-mixing efficiency	0.5
Ice-thickness distribution	triangular
Basal heat flux formula	$\rho_i C_w C_h U_i / \rho_w$

where ρ_i is ice density, ρ_w is water density, C_w is the volumetric heat capacity of water, C_h (= 0.006) is an empirical heat transfer coefficient, U_i (= 0.6 cm s^{-1}) is the friction velocity of ice, and ΔT is the elevation of the water temperature above freezing (from McPhee (1992)).

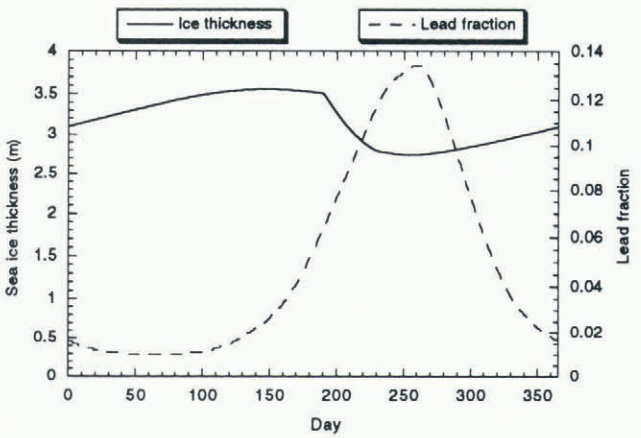

Fig. 1. The annual cycle of central Arctic sea-ice thickness and lead fraction in the control simulation.

The simulated sea ice is thickest at the end of May (3.56 m) and thins to a late-summer minimum of 2.74 m in mid-September. The mean annual thickness is 3.18 m, close to the observed estimates of Bourke and Garrett (1987). The predicted concentration of open water is smallest in February and March, but never reaches the minimum value of 0.5% allowed by the model, because of the divergence produced by the ice-export term. This behavior is in sharp contrast to a simulation with a leads parameterization by Vavrus (1995), in which the lack of ice export allowed significant thickening of ice by ridging once the minimum lead fraction was reached during winter. Open water becomes most widespread in mid-September (13%), the timing and magnitude of which agrees with observations, as does the phase and amplitude of the annual cycle of lead fraction (Asselin, 1977; Zakharov, 1987).

The predicted basal heat flux is 0 during the polar night and peaks at 8.4 W m^{-2} in mid-August. The mean annual value of 1.75 W m^{-2} is close to the inferred value around 2 W m^{-2} (Maykut and Untersteiner, 1971). The simulated maximum melt-pond fraction, which was formulated to match observed estimates, is 25%, and occurs in mid-July. The ice-surface temperature in the model drops to 240 K in January and February, and peaks at the melting point from late-June to late-August.

https://doi.org/10.3189/S0260305500013720 Published online by Cambridge University Press

SENSITIVITY TO PARAMETERIZATIONS

The uncertainty of how solar-energy absorption in the upper Arctic Ocean is actually partitioned between mixed-layer warming and ice melting has been raised in previous observational and modeling studies (Maykut and Perovich, 1987; Steele, 1992). Here the model is subjected to a range of possible partitionings to examine how sensitive the ice characteristics are to the choice of partitioning, and to assess which combinations produce the most realistic patterns of ice thickness and concentration. As outlined in the model description, an option exists for shutting off the model's prognostic partitioning of mixed-layer heat content and replacing it with prescribed fractions of the air–sea energy flux at the lead surface to warm the mixed layer and to melt the ice laterally. The results of this experiment are presented in Figure 2, which shows a pronounced non-linearity in the response of the mean annual ice thickness to changes in heat partitioning. If less than half of the energy entering the mixed layer is applied to heating, then reductions in this fraction (F_{HEAT}) cause substantial thickening of the ice. If a majority of the incoming energy goes toward heating, however, then only negligible variations in ice thickness occur when the heat partitioning changes. Because F_{HEAT} is a measure of the ocean–ice heat transfer, these results are consistent with those of Maykut and Untersteiner (1971), who showed that sea-ice thickness is more sensitive to decreases in the basal heat flux (especially at very low values) than to increases.

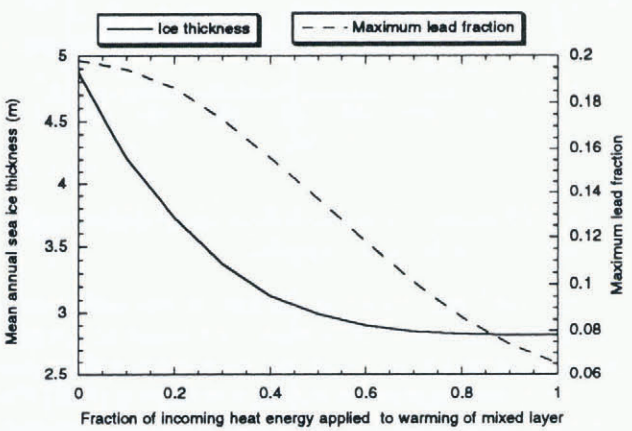

Fig. 2. The mean annual central Arctic sea-ice thickness (solid line) and maximum summertime lead fraction (dashed line) as a function of the fraction of atmospheric-heat energy entering the mixed layer that is used to warm the upper ocean. The remaining fraction is used to melt ice laterally.

The ice in this model thins even more gradually with increases in F_{HEAT}, however, because the basal heat flux parameterization allows only a fraction of the mixed-layer heat content to melt the ice bottom. The maximum summertime lead fraction displays a more linear decrease with increases in F_{HEAT}, as less energy is available for lateral melting. Note that there is still open water simulated, even with no lateral melting, owing to the effects of the prescribed ice-export term and the vertical meltoff of thin ice.

If one accepts that in the central Arctic the mean annual ice thickness is around 3 m (SHEBA, 1993) and that the maximum open-water fraction is about 0.15 (Asselin, 1977; Zakharov, 1987), then these results suggest that the energy gained by the upper ocean during summer goes almost equally toward heating and melting. This conclusion supports the ad hoc approach used in the sea-ice models of Mellor and Kantha (1989) and Hibler (1979), who used half of the mixed-layer heat content for lateral melting and half for heating of the ocean. The remainder of this paper describes the results of experiments in which the amount of lateral melting and mixed-layer warming are no longer prescribed, but are instead predicted by the model.

The mean ice thickness and the timing of open-water production are fairly insensitive to the amount of lateral mixing between water within leads and water beneath ice, as long as there is at least some mixing. Figures 3a and b illustrate the responses of the ice thickness to the prescribed fraction of complete lateral mixing (LATMIX) within the upper ocean, and to the prescribed fraction of complete vertical mixing (VERTMIX) within leads. Figure 3a shows the mean ice thickness when a control value of 0.5 for VERTMIX is fixed, while LATMIX is varied from 0 (no lateral mixing) to 1 (complete lateral mixing). When there is at least 4% of complete lateral mixing, then the ice thickness remains within a range of about 20 cm. The sea ice actually thickens slightly as LATMIX increases, even though enhanced mixing causes more of the solar energy absorbed by leads to reach the water beneath the ice and generate more vertical melting. The reason for this surprising response is that enhanced lateral mixing also forces the sub-ice mixed layer to lose its heat content more quickly once the cold season ensues.

Since leads lose heat rapidly to the overlying atmosphere beginning in early autumn, and because a large LATMIX allows easy energy exchange across the entire mixed layer, the extra heat gained by the sub-ice portion of the mixed layer with vigorous lateral mixing is quickly lost during the fall. This process results in reduced bottom melting, compared to cases with only slight lateral mixing. If the mixed layer becomes too stagnant, however (LATMIX <0.04), then virtually none of the solar energy absorbed by open water is available for bottom melting, and thus the ice thickens to an unrealistic maximum of almost 5 m for the limit of no lateral mixing. This limit is also unrealistic because, in this case, the open water concentration does not reach its maximum until late October, over one month later than observed.

Whether leads are well stratified or not makes virtually no difference to sea-ice characteristics (Fig. 3b). With LATMIX fixed at the control value of 1.0, variations of VERTMIX from 0–1 cause a <10 cm difference in the mean annual ice thickness, and virtually no difference in the timing of the peak lead fraction. It should be noted, however, that the lateral-melting rate in the parameterization used here depends on the energy absorbed by the upper lead during a time-step, rather than on the temperature difference between the upper lead and the adjacent ice. It would be physically more plausible to make the lateral-melt rate a function of the temperature difference, and in such a scheme the amount of vertical mixing within leads might be important. Unfortunately, this kind of parameterization is difficult to implement, owing to wide discrepancies in observed lateral-melt rates and the requirement of an (as yet unverifiable) ice-floe geometry distribution (Steele, 1992).

Given the amount of discussion in the literature regarding the best choice of a basal heat flux parameterization (e.g. Harvey, 1990; Steele, 1992), a surprising result of this

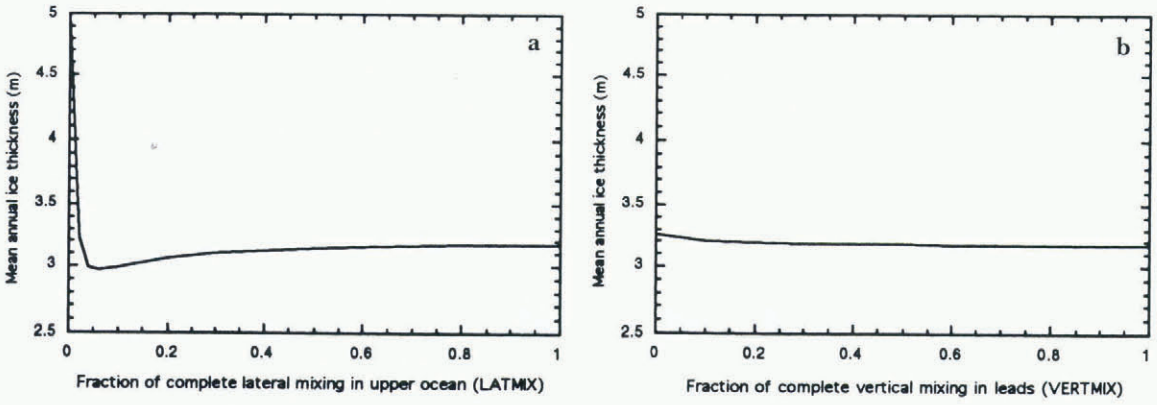

Fig. 3. The effect of (a) the lateral-mixing efficiency within the mixed layer (LATMIX) and (b) the vertical-mixing efficiency within leads (VERTMIX) on the mean annual sea-ice thickness.

study is how little the ice pack seems to depend on which approximation is used. Table 2 shows the results of three very different parameterizations. The control case uses the formula from McPhee (1992), which is based on a variety of measurements across the Arctic, and allows the mixed layer to exceed freezing point, consistent with observations (Maykut and McPhee, 1995). The second case uses only half this value, while the third case immediately applies all of the mixed-layer heating beneath the ice to bottom melting, an approximation frequently used in sea-ice models (e.g. Fifechet and Gaspar, 1988).

Table 2. The effect of heat flux parameterizations used in the experiments

Basal heat flux magnitude	Mean annual ice thickness	Maximum open water fraction and date	Mean annual basal heat flux
	m		W m^{-2}
Control value	3.18	0.134 (Sep. 17)	1.75
0.5 × control	3.38	0.133 (Sep. 21)	1.51
Maximum possible	3.05	0.135 (Sept. 12)	1.90

Although the mean annual ice thickness does differ, depending on the parameterization, the range is surprisingly small. As expected, the thinnest ice results when all of the heat energy is used to melt the ice, but this thickness differs by only about 10 cm from that obtained with the control parameterization, which uses only a small fraction of the available heat energy to melt the ice. The reason for the similar response is that the control parameterization allows the mixed layer to serve as a heat reservoir during the summer, and then slowly dissipates this energy in the form of enhanced bottom melting during the late-summer and fall, relative to the third case. This extra melting from below during autumn retards the rapid thickening of ice as the atmosphere is cooling, which results in a mean annual thickness quite close to the case with maximum bottom ablation. Note also that the choice of a basal heat flux parameterization has little effect on the timing or magnitude of the maximum open water amount during summer.

Traditionally sea-ice models have not used an ice-thickness distribution, instead treating the ice at a gridpoint as a single slab of a given thickness. Numerous observations from submarine sonar and ice platforms have shown, however, that ice packs consist of ice floes of various shapes and sizes (e.g. Wadhams and Horne, 1980; Tucker and others, 1992). In an attempt to account for this spatial variability, some models have included a prescribed ice-thickness distribution, in which the ice is assumed to be uniformly distributed between 0 and twice the mean thickness in a gridbox (Hibler, 1979; Harvey, 1988; Pollard and Thompson, 1994). When vertical ablation occurs, the fractional ice coverage is decreased to account for the meltoff of the thinnest floes (see Harvey (1988) for details). Although mathematically simple, the assumption of a uniform thickness distribution is at odds with most measurements from the Arctic and Antarctic (e.g. Tucker and others, 1992; Wadhams and others, 1987), which show only small amounts of very thin and very thick ice, but large amounts of ice near the mean local thickness. To incorporate this kind of observed distribution, the model described here prescribes that sea ice be distributed between the limits of 0 and twice the mean thickness, but with a triangularly shaped probability density function that peaks at the mean ice thickness, and falls to zero at the two limits.

The effect of the various distributions of the simulated ice characteristics is shown in Table 3. There is a strong similarity between the simulation with a triangular distribution and the one with a single slab of constant thickness, because very little thin ice exists in the former case and none exists in the latter. A uniform distribution causes much more open water during summer and a much thinner ice cover, due to the over-abundance of assumed thin ice floes and the resulting positive feedbacks that occur between melting and solar heating within the ice pack as the lead fraction increases.

Table 3. The effect of ice-thickness distributions used in the experiments

Ice-thickness distribution	Mean annual ice thickness	Maximum open water fraction and date	Mean annual basal heat flux
	m		W m^{-2}
Triangular	3.18	0.134 (Sept. 17)	1.75
Uniform	2.31	0.328 (Sep. 19)	3.14
None (single slab)	3.31	0.133 (Sep. 17)	1.61

https://doi.org/10.3189/S0260305500013720 Published online by Cambridge University Press

CONCLUSIONS

A 1-D sea-ice model of the central Arctic is used to assess the ice pack's sensitivity to a variety of parameterizations and processes. The advantages of this model over earlier sea-ice models include the inclusion of a melt-pond parameterization, improved treatment of leads, a more realistic ice-thickness distribution, and a sophisticated albedo parameterization. The results suggest that the solar energy absorbed in the mixed layer should be divided nearly evenly between warming of the water and lateral melting of the ice. As long as there is some lateral mixing within the mixed layer, then the exact amount does not strongly affect the ice thickness or concentration. The amount of vertical stratification within leads appears to be an even less important influence on the ice pack, as variations in vertical mixing ranging from complete to none, produced only slight differences in the simulated ice field.

The choice of the bottom-melting parameterization has surprisingly little effect on the ice thickness, at least for the present climate, because efficient conversion of oceanic-heat energy into bottom melting during summer depletes the mixed-layer heat content more rapidly, resulting in reduced basal heat fluxes during autumn. The type of ice-thickness distribution strongly affects the ice thickness and open water amount. It appears that the use of a uniform ice-thickness distribution will favor an ice pack that is too thin and sparse, as occurred in a recent atmospheric GCM simulation of the Arctic that used such an approximation (Pollard and Thompson, 1994).

Within the limitations of the model, these results may be useful for large-scale climate models that require a balance between sophisticated physics and computational efficiency. These simulations suggest that such models need not be very concerned with the amount of mixing in the upper ocean, nor even with the treatment of the basal heat flux. More consideration should be given to how much solar energy is used for lateral melting and to the choice of an ice-thickness distribution. A caveat to these conclusions is that they apply to the modern Arctic sea-ice pack; sensitivities to parameterizations may be quite different under altered climatic regimes, such as CO_2 doubling or paleoclimates.

ACKNOWLEDGEMENTS

This work was supported by a NASA Global Change Graduate Fellowship (NGT 30346).

REFERENCES

Alley, R. B. 1995. Resolved: the Arctic controls global climate change. *In* Smith, W.O. and J.M. Grebmeier, *eds. Arctic oceanography: marginal ice zones and continental shelves*. Washington, DC, American Geophysical Union, 263–283. (Coastal and Estuarine Series 49.)

Asselin, R. 1977. *Northern Hemisphere sea ice climatology and analyses*. Dorval, Que., Atmospheric Environment Service. Division de Recherche en Prévision Numérique.

Barry, R. G. 1983. Arctic Ocean ice and climate: perspectives on a century of polar research. *Ann. Assoc. Am. Geogr.*, **73**(4), 485–501.

Bourke, R. H. and R. P. Garrett. 1987. Sea ice thickness distribution in the Arctic Ocean. *Cold Reg. Sci. Technol.*, **13**(3), 259–280.

Curry, J. A., J. L. Schramm and E. E. Ebert. 1995. Sea ice–albedo climate feedback mechanism. *J. Climate*, **8**(2), 240–247.

Ebert, E. E. and J. A. Curry. 1993. An intermediate one-dimensional thermodynamic sea ice model for investigating ice–atmosphere interactions. *J. Geophys. Res.*, **98**(C6), 10,085–10,109.

Fifechet, T. and P. Gaspar. 1988. A model study of the upper ocean–sea ice interactions. *J. Phys. Oceanogr.*, **18**(2), 181–195.

Grenfell, T. C. 1979. The effects of ice thickness on the exchange of solar radiation over the polar oceans. *J. Glaciol.*, **22**(87), 305–320.

Grenfell, T. C. and G. A. Maykut. 1977. The optical properties of ice and snow in the Arctic Basin. *J. Glaciol.*, **18**(80), 445–463.

Harvey, L. D. D. 1988. Development of a sea ice model for use in zonally averaged energy balance climate models. *J. Climate*, **1**(12), 1221–1238.

Harvey, L. D. D. 1990. Testing alternative parameterizations of lateral melting and upward basal heat flux in a thermodynamic sea ice model. *J. Geophys. Res.*, **95**(C5), 7359–7365.

Hibler, W. D., III. 1979. A dynamic thermodynamic sea ice model. *J. Phys. Oceanogr.*, **9**(7), 815–846.

Hibler, W. D., III. 1984. The role of sea ice dynamics in modeling CO_2 increases. *In* Hansen, J. E. and T. Takahashi, *eds. Climate processes and climate sensitivity*. Washington, DC, American Geophysical Union, 238–253. (Geophysical Monograph 29, Maurice Ewing Series 5.)

Kutzbach, J. E., R. G. Gallimore and P. J. Guetter. 1991. Sensitivity experiments on the effect of orbitally-caused insolation changes on the interglacial climate of high northern latitudes. *Quat. Int.*, **10–12**, 223–229.

Manabe, S., R. J. Stouffer, M. J. Spelman and K. Bryan. 1991. Transient response of a coupled ocean–atmosphere model to gradual changes of atmospheric CO_2. Part I: Annual mean response. *J. Climate*, **4**(8), 785–818.

Maykut, G. A. and M. G. McPhee. 1995. Solar heating of the Arctic mixed layer. *J. Geophys. Res.*, **100**(C12), 24,691–24,703.

Maykut, G. A. and D. K. Perovich. 1987. The role of shortwave radiation in the summer decay of a sea ice cover. *J. Geophys. Res.*, **92**(C7), 7032–7044.

Maykut, G. A. and N. Untersteiner. 1971. Some results from a time-dependent thermodynamic model of sea ice. *J. Geophys. Res.*, **76**(6), 1550–1575.

McPhee, M. G. 1992. Turbulent heat flux in the upper ocean under sea ice. *J. Geophys. Res.*, **97**(C4), 5365–5379.

McPhee, M. G. and N. Untersteiner. 1982. Using sea ice to measure vertical flux in the ocean. *J. Geophys. Res.*, **87**(3), 2071–2074.

Mellor, G. L. and L. Kantha. 1989. An ice–ocean coupled model. *J. Geophys. Res.*, **94**(C8), 10,937–10,954.

Mitchell, J. F. B., S. Manabe, V. Meleshko and T. Tokioka. 1990. Equilibrium climate change — and its implications for the future. *In* Houghton, J. T., G. J. Jenkins and J. J. Ephraums, *eds. Climate change: the IPCC scientific assessment*. Cambridge, etc., Cambridge University Press, 131–172.

Morison, J. H. and J. D. Smith. 1981. Seasonal variations in the upper Arctic Ocean as observed at T-3. *Geophys. Res. Lett.*, **8**(7), 753–756.

Parkinson, C. L. and W. M. Washington. 1979. A large-scale numerical model of sea ice. *J. Geophys. Res.*, **84**(C1), 311–337.

Perovich, D. K. and G. A. Maykut. 1990. Solar heating of a stratified ocean in the presence of a static ice cover. *J. Geophys. Res.*, **95**(C10), 18,233–18,245.

Pollard, D. and S. L. Thompson. 1994. Sea-ice dynamics and CO_2 sensitivity in a global climate model. *Atmosphere-Ocean*, **32**(2), 449–467.

Semtner, A. J., Jr. 1976. A model for the thermodynamic growth of sea ice in numerical investigations of climate. *J. Phys. Oceanogr.*, **6**(5), 379–389.

SHEBA Science Working Group. 1993. *A report on the Surface Heat Budget of the Arctic Ocean (prospectus)*. Seattle, WA, University of Washington. Polar Science Center. ARCSS OAII Science Management Office.

Shine, K. P. and A. Henderson-Sellers. 1985. The sensitivity of a thermodynamic sea ice model to changes in surface albedo parameterization. *J. Geophys. Res.*, **90**(D1), 2243–2250.

Steele, M. 1992. Sea ice melting and floe geometry in a simple ice-ocean model. *J. Geophys. Res.*, **97**(C11), 17,729–17,738.

Tucker, W. B., III, D. K. Perovich, A. J. Gow, W. F. Weeks and M. R. Drinkwater. 1992. Physical properties of sea ice relevant to remote sensing. *In* Carsey, F. D. *and 7 others, eds. Microwave remote sensing of sea ice*. Washington, DC, American Geophysical Union, 9–28. (Geophysical Monograph Series 68.)

Vavrus, S. J. 1995. The sensitivity of the Arctic climate to leads in a coupled atmosphere–mixed- layer ocean model. *J. Climate*, **8**(2), 158–171.

Wadhams, P. and R. J. Horne. 1980. An analysis of ice profiles obtained by submarine sonar in the Beaufort Sea. *J. Glaciol.*, **25**(93), 401–424.

Wadhams, P., M. A. Lange and S. F. Ackley. 1987. The ice thickness distribution across the Atlantic sector of the Antarctic Ocean in midwinter. *J. Geophys. Res.*, **92**(C13), 14,535–14,552.

Washington, W. M. and G. A. Meehl. 1984. Seasonal cycle experiment on the climate sensitivity due to a doubling of CO_2 with an atmospheric general circulation model coupled to a simple mixed layer ocean. *J. Geophys. Res.*, **89**(D6), 9475–9503.

Wilson, C. A. and J. F. B. Mitchell. 1987. A doubled CO_2 climate sensitivity experiment with a GCM including a simple ocean. *J. Geophys. Res.*, **92**(D11), 13,315–13,343.

Zakharov, V. F. 1987. Morskiye l'dy i klimat [Sea ice and climate]. *In* Kotlyakov, V. M. and M. G. Grosval'd, *eds. vzaimodeystviye oledeneniya s atmosferoy i okeanom [Interactions between glaciation, atmosphere and ocean]*. Moscow, Nauka, 66–89.